

Dynamic lock-in compensation for mechanically dithered ring laser gyros

Zhenfang Fan (樊振方), Hui Luo (罗晖)*, Guangfeng Lu (卢广锋), and Shaomin Hu (胡绍民)

College of Optoelectronic Science and Engineering, National University of Defense Technology, Changsha 410073, China

*Corresponding author: luohui.luo@163.com

Received August 23, 2011; accepted December 12, 2011; posted online March 15, 2012

In ring laser gyros (RLGs), dynamic lock-in, which results from information loss in the lock-in region, occurs when a constant sine bias is introduced. However, sampling some signals in the lock-in region for a particular duration allows the retrieval of lost information. It is demonstrated how dynamic lock-in and the flat region in the input-output curve near the zero angle rate can be eliminated after compensation.

OCIS codes: 140.3370, 140.3430, 230.5160.

doi: 10.3788/COL201210.061403.

Ring laser gyros (RLGs) have more advantages than traditional spinning-mass gyros. The operation principle of a RLG involves the Sagnac effect^[1,2]. The laser cavity supports two independent waves traveling toward opposite directions. When an angle rate is introduced, the oscillation frequencies of the two beams differ. Thus, the angle rate can be measured by detecting the frequency difference. The RLG is, in fact, a ring laser whose gain media is He-Ne gas^[3].

The lock-in phenomenon can significantly constrain the performance of the RLG^[4-7]. Lock-in is caused by the mutual coupling between the opposite traveling waves^[8-11]. With a low angle rate input, both waves lock to a common frequency, and the gyro becomes unresponsive to the input.

The lock-in effect can be avoided by introducing a mechanical dither and placing the gyro far from the lock-in region most of the time^[12]. The gyro that works in this manner is often called a “mechanically dithered ring laser gyro”^[13]. However, if a pure sine wave dither is introduced, dynamic lock-in may occur. In other words, if the angle rate is below the dynamic lock-in threshold, the output also becomes zero^[14] and a flat region near the zero input angle rate appears. Dynamic lock-in is the same as regular lock-in, except that the value is much smaller.

Previous studies have indicated that dynamic lock-in is mainly caused by information loss during lock-in traversal^[15,16]. Information loss is related to the phase of the beat frequency signal and angle acceleration in the zero rate point^[17]. This letter successfully compensates dynamic lock-in by sampling the signals in the zero rate point.

The phase equation of a RLG can be written as

$$\frac{d\psi}{dt} = \Omega_i + \Omega_L \cos(\psi), \quad (1)$$

where ψ is the phase of the beat frequency signal, Ω_i is the input angle rate, and Ω_L is the lock-in threshold, which must be positive. If $|\Omega_i| \leq \Omega_L$, Eq. (1) has the following stationary solution:

$$\sin \psi = \frac{\Omega_i}{\Omega_L}, \quad (2)$$

where the mean output is zero.

If $|\Omega_i| > \Omega_L$, the average frequency of ψ can be obtained. Changing the form of Eq. (1) yields

$$\frac{1}{\Omega_i + \Omega_L \cos(\psi)} d\psi = dt. \quad (3)$$

Take integration of ψ over $[0, 2\pi]$; the mean period T can be obtained as

$$T = \int_0^{2\pi} \frac{1}{\Omega_i + \Omega_L \cos(\psi)} d\psi = \frac{2\pi}{\sqrt{\Omega_i^2 - \Omega_L^2}}. \quad (4)$$

The average frequency of the beat frequency signal is

$$\omega_a = \frac{2\pi}{T} = \sqrt{\Omega_i^2 - \Omega_L^2}. \quad (5)$$

In Fig. 1, the response curve with the lock-in threshold is represented by the green line, whereas the ideal response curve without lock-in is denoted by the red line.

When a sine dither is introduced, Eq. (1) can be written as

$$\dot{\psi} = \Omega_i + \Omega_d \sin(\omega_d t) + \Omega_L \cos(\psi), \quad (6)$$

where Ω_d is the peak dither angle rate and ω_d is the dither frequency. Although the gyro works outside the lock-in region most of the time, it must traverse the lock-in region twice every dither cycle, resulting in the dynamic

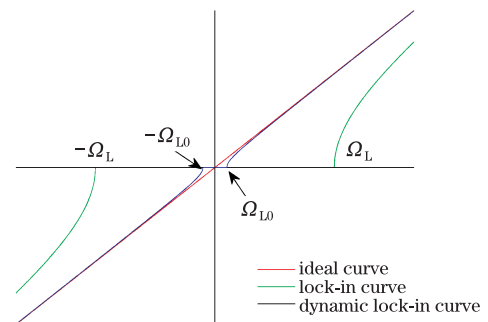


Fig. 1. (Color online) Lock-in and dynamic lock-in of the RLG.

lock-in phenomenon. Chow derived the mean frequency solution near the zero input angle rate in Eq. (6) as

$$\dot{\psi} = \Omega_i + \Omega_L J_0 \left(\frac{\Omega_d}{\omega_d} \right) \cos(\psi), \quad (7)$$

where J_0 is the zero-order Bessel function. Assuming that

$$\Omega_{L0} = \Omega_L J_0 \left(\frac{\Omega_d}{\omega_d} \right), \quad (8)$$

Eq. (7) can be written as

$$\dot{\psi} = \Omega_i + \Omega_{L0} \cos(\psi). \quad (9)$$

In Eq. (8), Ω_d/ω_d is often large. Thus, according to the characteristic of the Bessel function, $J_0 \left(\frac{\Omega_d}{\omega_d} \right) \ll 1$ and $\Omega_{L0} \ll \Omega_L$, indicating that, after the sine wave bias, the origin lock-in threshold Ω_L has been changed into the dynamic lock-in threshold Ω_{L0} . If $|\Omega_i| \leq \Omega_{L0}$, the mean output is zero. According to the analysis above, if $|\Omega_i| > \Omega_{L0}$, the average frequency of the beat frequency signal is

$$\omega_a = \sqrt{\Omega_i^2 - \Omega_{L0}^2}. \quad (10)$$

The response with the sine wave is represented by the blue line in Fig. 1.

The lock-in is a result of information loss during lock-in traversal. By using a parabolic approximation, when the direction changes from clockwise (CW) to counterclockwise (CCW), the phase error can be expressed as^[18]

$$\Delta E^+ = \Omega_L \sqrt{\frac{2\pi}{\ddot{\psi}^+}} \cos \left(\psi_0^+ + \frac{\pi}{4} \right), \quad (11)$$

where ψ_0^+ is the phase in the direction change from CW to CCW and $\ddot{\psi}^+$ is the phase acceleration. When the direction changes from CCW to CW, the phase error can be expressed as

$$\Delta E^- = \Omega_L \sqrt{\frac{2\pi}{\ddot{\psi}^-}} \cos \left(\psi_0^- + \frac{\pi}{4} \right), \quad (12)$$

where ψ_0^- is the phase in the direction change from CCW to CW and $\ddot{\psi}^-$ is the phase acceleration. In fact, the phase of the beat frequency signal ψ cannot be obtained directly. In the readout structure, two photodiodes, which are in quadrature to each other, are assembled to obtain the output signal of the RLG. Assuming that the phase sensed by one of the photodiodes is ψ_H , the phase sensed by the other photodiode must be $\psi_H + \frac{\pi}{2}$. The relationship between ψ and ψ_H can be expressed as

$$\psi = \psi_H + \varepsilon, \quad (13)$$

where ε is a constant bias angle. Substituting Eq. (13) into (11) yields

$$\begin{aligned} \Delta E^+ &= \Omega_L \sqrt{\frac{2\pi}{\ddot{\psi}^+}} \cos \left(\varepsilon + \frac{\pi}{4} \right) \cos \psi_{H0+} \\ &\quad - \Omega_L \sqrt{\frac{2\pi}{\ddot{\psi}^+}} \sin \left(\varepsilon + \frac{\pi}{4} \right) \sin \psi_{H0+}. \end{aligned} \quad (14)$$

Moreover, substituting Eq. (13) Eq. (12) yields

$$\begin{aligned} \Delta E^- &= \Omega_L \sqrt{\frac{2\pi}{\ddot{\psi}^-}} \cos \left(\varepsilon + \frac{\pi}{4} \right) \sin \psi_{H0-} \\ &\quad + \Omega_L \sqrt{\frac{2\pi}{\ddot{\psi}^-}} \sin \left(\varepsilon + \frac{\pi}{4} \right) \cos \psi_{H0-}. \end{aligned} \quad (15)$$

Under static conditions

$$\ddot{\psi}^+ = \ddot{\psi}^- = \ddot{\psi}, \quad (16)$$

the above equation is satisfied. Assuming that

$$\begin{aligned} a &= \Omega_L \cos \left(\varepsilon + \frac{\pi}{4} \right), \\ b &= \Omega_L \sin \left(\varepsilon + \frac{\pi}{4} \right), \end{aligned} \quad (17)$$

in a dither cycle, the error accumulation can be expressed as

$$\begin{aligned} \Delta E &= \Delta E^+ + \Delta E^- = a \sqrt{\frac{2\pi}{\ddot{\psi}}} (\cos \psi_{H0+} + \sin \psi_{H0-}) \\ &\quad + b \sqrt{\frac{2\pi}{\ddot{\psi}}} (-\sin \psi_{H0+} + \cos \psi_{H0-}). \end{aligned} \quad (18)$$

Moreover, assuming that

$$\begin{aligned} P1 &= \sqrt{\frac{2\pi}{\ddot{\psi}}} (\cos \psi_{H0+} + \sin \psi_{H0-}), \\ P2 &= -\sqrt{\frac{2\pi}{\ddot{\psi}}} (\sin \psi_{H0+} + \cos \psi_{H0-}), \end{aligned} \quad (19)$$

Eq. (18) can be expressed as

$$\Delta E = aP1 + bP2. \quad (20)$$

Equation (20) cannot be evaluated because both a and b are related to Ω_L and ε , which cannot be measured directly. However, in short periods, both Ω_L and ε can be considered as constants. Therefore, both a and b can be considered as unknown constants and weights of $P1$ and $P2$. For a sine wave bias, the phase acceleration $\ddot{\psi}$ can also be considered as a constant. $P1$ and $P2$ can be obtained by using a high-speed signal processing technique.

As mentioned earlier, the root cause of dynamic lock-in is information loss, which was expressed in Eq. (20). Thus, if Eq. (20) can be evaluated, then dynamic lock-in can be compensated. The key point is to obtain the values of a and b . In Ref. [18] a curve-fitting method was proposed to obtain the values of a and b . In this method, when the lock-in error is compensated, the output of the RLG will have minimum variance. This conclusion is reasonable when the gyro is not in the dynamic lock-in region, because only a zero output can be obtained in this region. The dynamic lock-in compensation can be realized in the following steps.

Step 1: The gyro is warmed up for about 5 h after startup to ensure that both Ω_L and ε have constant values.

Step 2: The gyro is placed outside the dynamic lock-in region. The curve-fitting method is then used to obtain a and b .

Step 3: The gyro is placed inside the dynamic lock-in region under different input angle rates. The output without compensation, as well as the $P1$ and $P2$ values, of the RLG is then recorded.

Step 4: The lock-in error compensation in Eq. (20) is applied using the values of a and b obtained in Step 2.

The gyro is placed in the rotary table as shown in Fig. 2.

The gyro and input axis are placed perpendicular and parallel to the Earth's surface, respectively. By changing the angular position of the rotary table, the input, which is the projection of the Earth's rotation, can be changed. The local latitude is 22.2° , and the angle rate of the Earth is $15^\circ/h$. Therefore, the maximum input angle rate of the gyro is

$$15^\circ/h \cdot \cos(22.2^\circ) = 13.888^\circ/h. \quad (21)$$

By changing the position of the rotary table, the input angle rate can be changed from $-13.888^\circ/h$ to $13.888^\circ/h$. The scale factor of the RLG is $1.8655^\circ/h/Hz$, and its maximum output is

$$13.888^\circ/h/1.8655^\circ/h/Hz = 7.445 \text{ Hz}. \quad (22)$$

Therefore, the output of the RLG can be changed from -7.445 to 7.445 Hz. When the input axis is in the east-west direction, the input angle rate is zero. The gyro is biased with a pure sine dither with a frequency of 389 Hz. Changing the position of the rotary table and watching the output response yields the response curve with dynamic lock-in shown in Fig. 3.

Using the lock-in compensation described in the four steps listed above, the dynamic lock-in curve in Fig. 3 can be compensated, and the result is shown in Fig. 4.

Figure 4 illustrates that, after compensation, the dynamic lock-in region in Fig. 3 disappears and the response curve becomes nearly a straight line. The curve after compensation seems to be imperfect, which may be

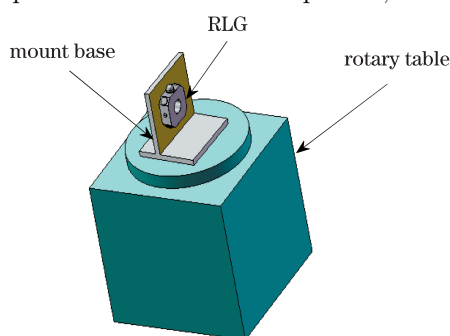


Fig. 2. Experimental setup.

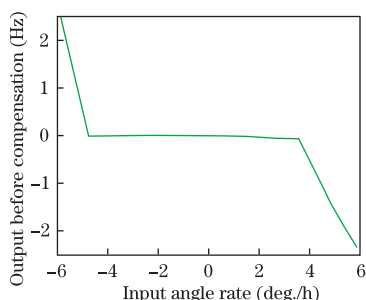


Fig. 3. Experimental dynamic lock-in response curve.

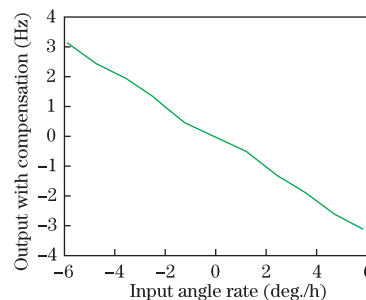


Fig. 4. Response curve after dynamic lock-in compensation.

caused by two reasons. Firstly, the compensation may introduce a new random noise in evaluating the information during lock-in traversal. Secondly, the lock-in equation shown in Eq. (1) cannot fully describe the mechanism of the RLG.

In conclusion, dynamic lock-in occurs when a pure sine dither bias is introduced into the RLG. This dynamic lock-in is generated by the information loss during the lock-in traversal. However, it is compensated by retrieving the appropriate information in the lock-in region. Although the response curve after compensation is imperfect, evidently, the flat region near the zero input angle rate can be removed.

This work was supported by the Program for New Century Excellent Talents in Universities (2010).

References

1. E. J. Post, *Re. Mod. Phys.* **39**, 475 (1967).
2. J. R. Wilkinson, *Prog. Quantum Electron.* **11**, 1 (1987).
3. G. Z. Xiao, X. W. Long, B. Zhang, and G. Li, *Chin. Opt. Lett.* **9**, 101201 (2011).
4. J. D. Cresser, W. H. Louisell, P. Meystre, W. Schleich, and M. O. Scully, *Phys. Rev. A* **25**, 2214 (1982).
5. B. L. Gao, *Journal of NUDT (in Chinese)* 1-36 (1979).
6. F. Aronowitz, "Theory and operation of a traveling-wave laser" PhD. Thesis (New York University, 1969).
7. F. Aronowitz, *J. Appl. Phys.* **41**, 130 (1970).
8. H. A. Haus, *J. Quantum Electron.* **21**, 78 (1985).
9. L. N. Mengozzi and W. E. Lamb, *Phys. Rev. A* **8**, 2103 (1973).
10. R. J. C. Spreeuw, R. Centeno, and N. J. van Druten, *Phys. Rev. A* **42**, 4315 (1990).
11. R. Rodloff, *IEEE J. Quantum Electron.* **23**, 438 (1987).
12. J. E. Killpatrick, "Laser angular rate sensor," U.S. patent 3, 373, 650 (April 2, 1965).
13. J. X. Tang, "Research and Design for Dither Bias System of Mechanically Dithered Ring Laser Gyroscopes" (in Chinese) PhD. Thesis (National University of Defense Technology, 2000).
14. W. W. Chow, *Rev. Mod. Phys.* **57**, 61 (1985).
15. D. Loukianov, *Optical Gyros and their Application (DTIC Document, 1999)*.
16. A. A. Morgan and G. R. Quasius, "Ring laser gyro system," U.S. patent 4,529,311 (Jul. 16, 1985).
17. H. A. Gustafson, W. L. Lim, and F. H. Zeman, "Ring Laser Lock-in Correction Apparatus," U.S. patent 4,641,970 (Feb. 10, 1987).
18. Z. Fan, H. Luo, S. Hu, and G. Xiao, *Opt. Eng.* **50**, 034403 (2011).